THE INFLUENCE OF INTAKE ACOUSTICS ON THE PERFORMANCE AND NOISE OF GASOLINE ENGINES

M.F. Harrison Cranfield University, School of Engineering, Cranfield, Beds, MK43 0AL
P.T. Stanev Cranfield University, School of Engineering, Cranfield, Beds, MK43 0AL

1. INTRODUCTION

Naturally aspirated gasoline engines produce noise. Some of this is radiated from the point of air ingestion and is known as intake orifice noise. The levels and spectra of intake orifice noise are functions of engine size, geometry, and operating conditions as well as the geometry of the intake system. The performance obtained from the engine is also a function of these:

$$T = \frac{\eta_f \, \eta_v N \, V d \, Q_{HV} \; \rho_{ai} \left(F/A\right)}{4\pi} \tag{1}$$

T = torque (Nm)
η_f = fuel conversion efficiency
η_v = volumetric efficiency
V_d = swept volume of the engine (m^3)
N = revolutions of the crankshaft per second
Q_{HV} = heating value (lower) of the fuel (Jkg^{-1})
ρ_{ai} = inlet air density (kgm^{-3})
F/A = fuel-air ratio

With respect to engine breathing, the torque obtained is proportional to the product $\eta_v \rho_{ai}$. In the naturally aspirated engine ρ_{ai} mostly depends on the prevailing atmospheric conditions with a secondary influence obtained from the cooling due to evaporation of the fuel charge. The volumetric efficiency is a measure of the mass flow of air obtained per unit swept volume of the engine:

$$\eta_v = \frac{2\dot{m}_{ai}}{V_d \; \rho_{ai} \; N} \tag{2}$$

$\dot{m}_{ai}$ = inlet air mass flow rate (kgs^{-1})

The volumetric efficiency is a function of engine geometry and engine speed, and from equation 2 it is clearly proportional to the rates of mass flow through the intake valve. Inflow to the cylinder will take place when the intake valve is open and there is a higher pressure in the port than in the cylinder. This favourable pressure ratio can be obtained either by causing reduced pressure in the cylinder with a downward moving piston or by causing raised pressure in the intake port using an acoustic wave. In the practical engine, both of these mechanisms are at work.

An attempt has been made to separate these two mechanisms in order to understand the intake process better. We will consider the reduced pressure caused by the moving piston first.

Assuming a wide open throttle we can write the approximate relationship:

$$\dot{V}_{ai}\left(m^3/s\right) \approx \frac{dV_d}{dt} \times \frac{S_v(t)}{S_p(t)} \tag{3}$$

$\dot{V}_{ai}$ = inlet air volume velocity (m^3/s) = $\frac{\dot{m}_{ai}}{\rho_{ai}}$
S_V = flow area under intake valve (m^2)
S_p = cross sectional area of intake port (m^2)

which is approximately equal to:

$$\eta_v \approx \frac{1}{V_d}\int_{IVC}^{IVO} \dot{V}_{ai}\, dt \tag{4}$$

IVO = intake valve open (time equivalent of degrees of crankshaft rotation)
IVC = intake valve closed

For a given engine and valve geometry, $\dot{V}_{ai}$ and hence η_v will rise linearly with engine speed. There is a natural limit to this, being the engine speed at which the flow through the valve or the port becomes sonic and the intake flow begins to choke.

The volumetric efficiency due to the effects of the moving piston computed using equation 4 will tend to be less than the 75-105% typically measured. It seems fair to assume that most of the difference is due to the effects of the acoustic wave causing a raised pressure in the intake port and thus a pressure drop across the intake valve that is more favourable to flow into the cylinder.

It is commonly known that, for a given intake geometry, certain engine speeds cause the formation of intense sound waves in the intake port, which if phased to coincide with the period just before IVC can increase η_v by 15% [1]. Intense sound waves in the intake port are radiated as intense intake orifice noise and thus a link between levels of engine performance and intake orifice noise is found.

This paper explores the links between inflow to the cylinder caused by the moving piston, inflow to the cylinder caused by intense sound waves in the intake port and the subsequently intense intake orifice noise. This is achieved by constructing the acoustic model described in the next section.

2. A LINEAR ACOUSTIC MODEL FOR THE INTAKE PROCESS

For this work, the intake process is described using a linear plane wave acoustic model. This is in contrast to the time marching, iterative gas dynamic schemes more commonly used to predict engine performance [2].

The model is shown in Figure 1. The intake process is modelled as a volume source V_S with associated source impedance Z_e, to which an acoustic load Z_1 is attached. The acoustic wave in the intake port is denoted as P_1.

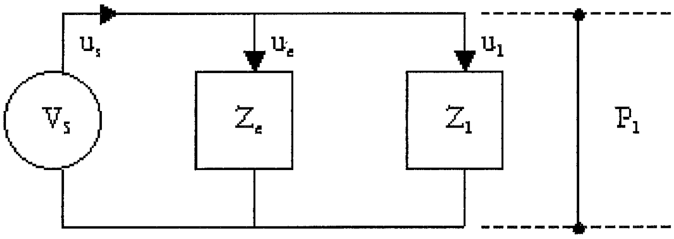

Figure: 1 An acoustic model for the intake process in a gasoline engine

The strength of the volume source is the volume velocity through the intake valve. This source strength is therefore related to volumetric efficiency as described in the introduction and hence is subject to both the effects of the moving piston and to the action of acoustic waves in the port (P_1). As V_S is dependent in part on P_1 the acoustic source and the acoustic load must be coupled.

Solving such a coupled system is difficult and requires an iterative approach. The advantage of the gas-dynamic schemes commonly used for this [2] is that the iteration is provided for by making calculations over several engine cycles and seeking convergence of the solution. The disadvantage of these schemes is that they don't allow the user much insight into the physical processes at work in the engine.

The acoustic model would provide insight into the physics of the problem but only if the coupled source and load may be described analytically or empirically without an iterative procedure. Equation 3 provides an analytic model for the source strength but in that case the source and load terms are uncoupled.

Experimental observation has shown that in the first half of the intake process, the true volume velocity time history matches that given by equation 3 fairly well. In the closing parts, the true volume velocity follows an empirical relationship given by equations 5,6

$$\int_{IVC}^{IVO} S_v \, \rho_{ai} \, K = \frac{2\dot{m}_{ai}}{N} \quad (5) \quad \text{and} \quad \dot{V}_s = KS_v \quad (6)$$

A calculation procedure has been developed where $\dot{V}_s$ is first calculated using equation 3. Subsequently, a value of the constant of proportionality K is found so that the maximum value of $\dot{V}_s$ obtained from equation 6 matches the maximum obtained from equation 3. The time history of $\dot{V}_s$ obtained in this way from equation 6 has been found to agree fairly well with experimental observation of true volume velocities through the valve and hence can be used as a model for the coupled source / load strength.

Having obtained a model for the coupled source strength, models are now required for the source and load impedances respectively. The load impedance Z_1 is simply the acoustic impedance of the intake duct at a point in the intake port just behind the valve. As such it may be calculated using established linear plane wave acoustic models [3]. The load impedance is effectively time invariant as long as the Mach number of the unsteady intake flow is fairly low. The source impedance Z_e however varies strongly with time, being near infinite when the valve is closed and rather different when the valve is open. As a simplifying assumption, the source impedance is taken here to be very high at all times and so the fluctuating pressure in the intake port, P_1 , is taken to be a function solely of V_s and Z_1.

3. EXPERIMENTAL INVESTIGATIONS

The realism of such a linear acoustic model has been investigated using a set of experiments performed on a Ricardo E6 single cylinder variable compression ratio engine in the configuration shown in Figure 2.

The engine was fitted with a rather long intake pipe (1.4m) and a fixed-venturi carburettor 400mm from the intake valve. A large airbox was used along with an orifice plate to measure air consumption rates. Pressure sensors were mounted in the cylinder, in the intake port and in the intake duct.

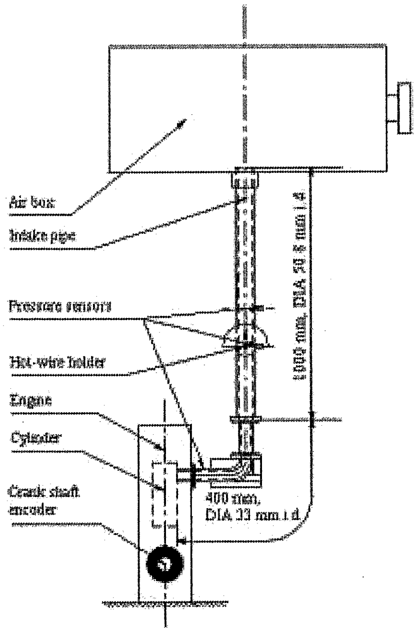

Figure: 2 Ricardo E6 single cylinder engine.

Figure 3 shows the fluctuating pressure in the intake port at around 2000 revmin^{-1}. The intake valve opens (IVO) at 352^0 after top dead centre (firing) and closes again (IVC) at 573^0 after top dead centre (firing). Results are shown when the engine is running under its own power and when it is being motored by the dynamometer. The motoring is obtained by switching off the ignition module that operates the spark plug and letting the dynamometer take over in speed control mode.

The results in Figure 3 show several things. Firstly the amplitude of the pressure wave is significant (10% of atmospheric pressure or a sound pressure level of 175 dB). Secondly there is a particular shape to the pressure trace: a depression after the valve first opens followed by a pressure maximum near the point of valve closing and a decaying oscillation once the valve is closed. Thirdly, firing rather than motoring the engine only has a small effect on the intake wave, and this is only when the valve is open. This is perhaps surprising given that when firing, the temperature of the in-cylinder gas during the exhaust stroke that immediately precedes the intake is as much as 1200K whereas when motoring it is only 400K. In effect, the low temperature during the exhaust stroke restricts the scavenging efficiency of the engine and is responsible for a small flow reversal from the cylinder to the intake port soon after IVO and the resulting small pressure peak seen near IVO in Figure: 3. Notwithstanding these small differences, the measured volumetric efficiency when motored (89.7%) is indistinguishable from that obtained when the engine is fired (89.9%).

This suggests that the intake process is only weakly affected by the in-cylinder gas temperatures that precede IVO.

As a result, the remaining experimental results shown in this paper are for a motored engine rather than a firing engine.

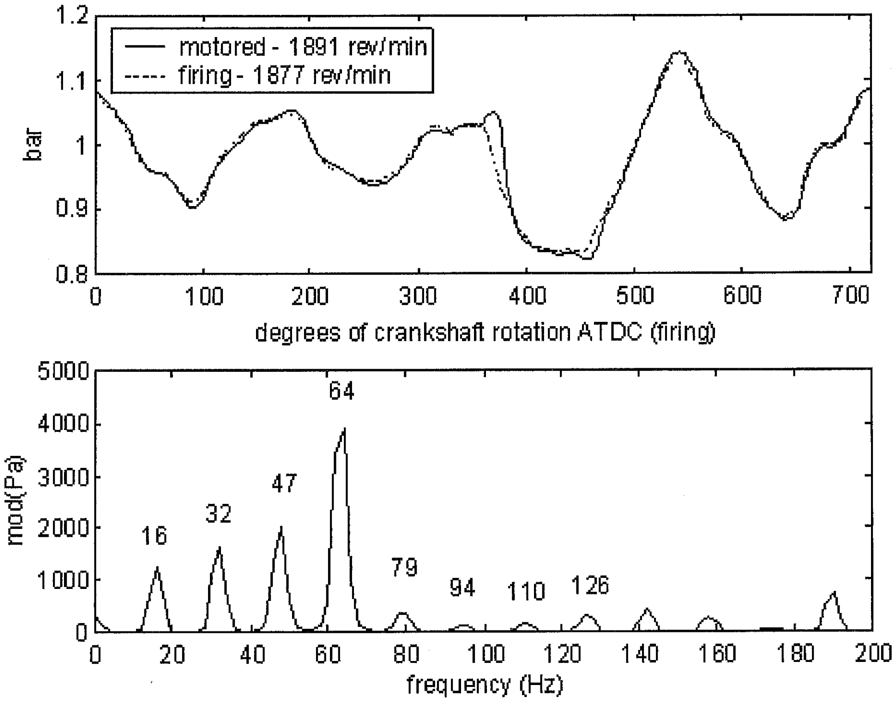

Figure: 3 Intake port pressures at around 2000 revmin^{-1}. Motored volumetric efficiency is 89.7%, firing is 89.9%

The spectrum of the motored intake port pressure is also shown in Figure 3. This has spectral components at all integer multiples of the 16 Hz cyclic frequency. The dominant 64 Hz component originates mostly from the period of decaying oscillation between IVC and the IVO for the next cycle.

Results obtained at other operating speeds show similar spectra but important differences occur. Firstly, the spectral levels vary in proportion with engine speed and hence in proportion with the source strength caused by the moving piston (equation 3). Secondly, the frequency at which the dominant spectral peak occurs does vary but only slightly between speeds. Closer inspection revels that it is always an integer multiple of the cycle frequency and that the frequency is always around 60Hz for this engine but it is not always the same harmonic of the cycle frequency.

4. CALCULATIONS

Why the pressure wave should oscillate at different harmonics of the cyclic frequency (the third harmonic in the case shown in Figure: 3) at different speeds has been investigated. Figure 4 shows the specific acoustic impedance ratio (ξ) in the straight portion of the intake pipe, 1m from the airbox:

$$\xi = \frac{ZS_p}{\rho_0 c_0} = \frac{1}{\rho_0 c_0}\left(\frac{P}{u}\right) \qquad (7)$$

c_0 = stagnation sound speed (ms^{-1})
P = acoustic pressure (Pa)
u = acoustic particle velocity (ms^{-1})
ρ_0 = stagnation density (kgm^{-3})

The theoretical results were obtained using established linear plane wave acoustic models [3]. The measurement of the impedance was undertaken using a two-transducer wave decomposition technique [4] on the motored engine. In this technique the acoustic field in the intake pipe is described as the sum of the positive and negative wave components p_1^+ and p_1^- respectively and is described by the equation

$$FFT\ (P_1) = p_1^+ e^{i(\omega t - \beta_1^+ x)} + p_1^- e^{i(\omega t + \beta_1^- x)} \qquad (8)$$

$$\beta = \text{complex wavenumber } = \left(\frac{\omega}{c}\right) - i\alpha \qquad (9)$$

where ω is the radial frequency ($rads^{-1}$), α is a visco-thermal attenuation coefficient and x is the distance away from a given plane in the pipe. With two pressure transducers in the intake pipe, at a short but known distance apart, a pair of simultaneous equations may be created with the form shown in equation 8. These can be solved algebraically to yield p_1^+ and p_1^- and hence

$$r = \frac{p^-}{p^+} \quad (10) \qquad\qquad \zeta = \frac{1+r}{1-r} \quad (11)$$

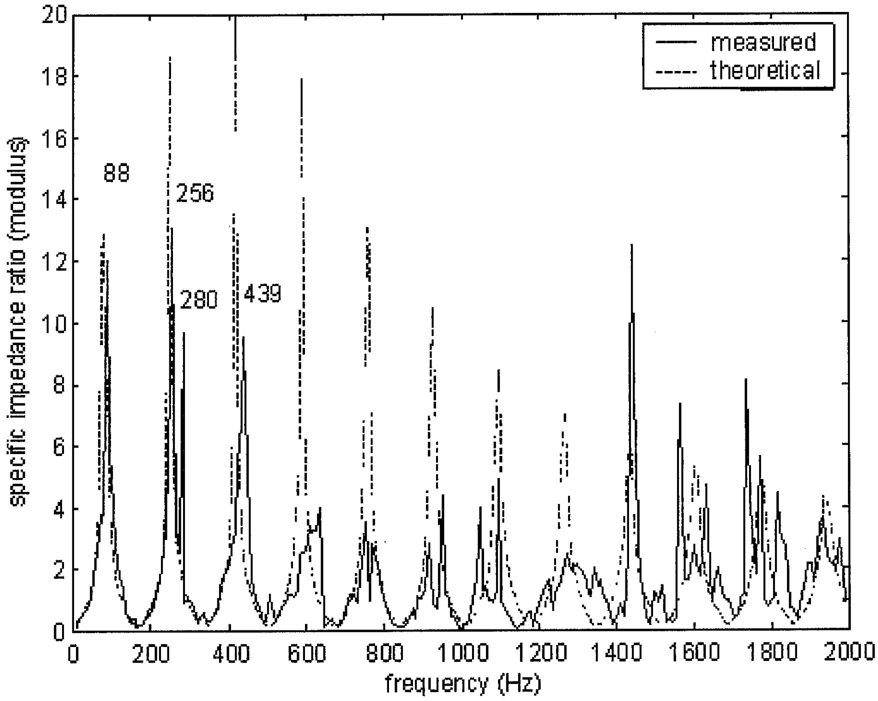

Figure: 4 Two-transducer wave decomposition results in the 1m pipe at 2000 revmin^{-1}. The peaks in the theoretical results occur at frequencies that are 3-9% lower than those measured.

The peaks in ζ correspond to acoustic resonances in the 1m pipe length. The frequencies at which they occur in the measured data (88, 256, 280, 439 Hz) can be predicted from the simple relationship:

$$f_r = \frac{n c_o}{4x} \tag{12}$$

x = 1m
n = 1, 3, 5...
c_o = 343 m/s

and (12) yields resonant frequencies at 86Hz, 257Hz, 429 Hz. The peaks in the measured data occur at frequencies that are 3-9% higher than those given by the theory. This suggests that the effective acoustic length of the pipe is perhaps some 6% shorter than its physical length in this case. Given the use of an airbox and a variable cross section for the pipe this is not surprising.

The physical length of the intake pipe from airbox to valve is 1.4m. Subtracting 6% of its length gives a length of 1.31m. The theoretical impedance spectrum for such a pipe is shown in Figure 5. The impedance spectrum in Figure 5 is used to represent the acoustic load Z_1 in the acoustic model shown in Figure 1.

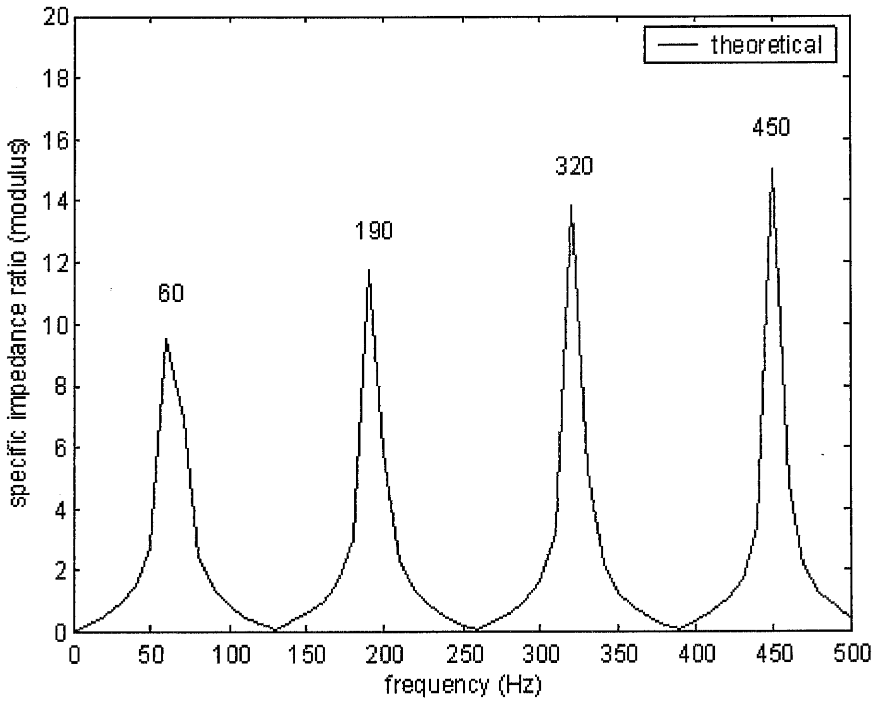

Figure: 5 Theoretical impedance for a 1.31m pipe.

The source strength V_S in the acoustic model is estimated using equation 6 and results are shown in Figure 6.

The frequency resolution of V_S is chosen to match precisely that of Z_1. As a result, the pressure time history in the intake port may be calculated thus:

$$P(t) = IFFT\left\lfloor \zeta_1(f)\, \rho_0\, c_0\, V_s(f)/S_p \right\rfloor \quad (13)$$

and the results are shown in Figure 7.

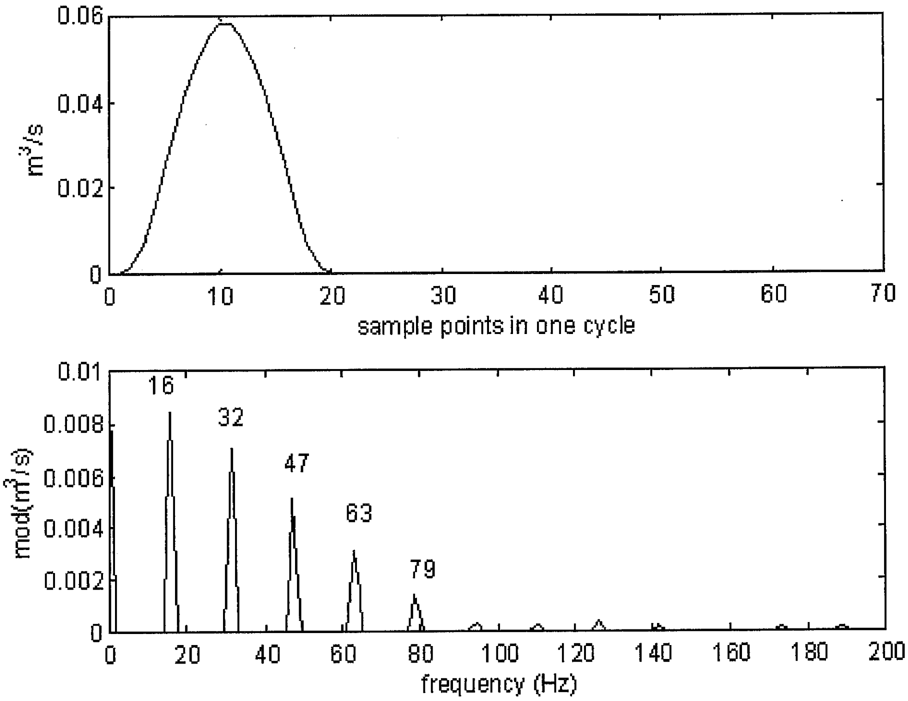

Figure: 6 Calculated source strength V_s at 2000 revmin^{-1}.

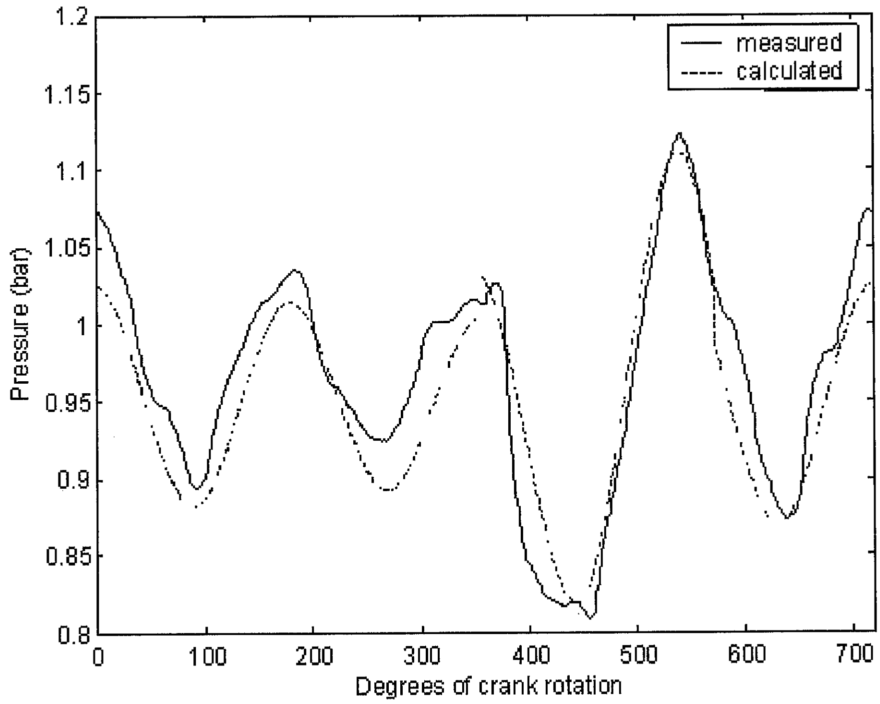

Figure: 7 Calculated and measured port pressures P_1 at 2000 revmin^{-1}.

The acoustic model produces a port pressure time history that agrees well with measurement (Figure 7). Therefore, it could be used to produce an intake port pressure time history to use as a starting point in a step-wise calculation of the flow through the valve using the common gas dynamic models [2]. The acoustic model also produces a good prediction of intake noise in its own right (Figure 8).

This calculation procedure aids the understanding of the engine breathing process. The source strength V_S has spectral components at all integer multiples of the cycle frequency but the lowest frequency components have the highest energy. The load impedance has resonant frequencies corresponding to odd numbers of ¼ wavelengths in the pipe (as determined by applying x=1.31m to equation 12 and comparing the resonant frequencies with those in Figure: 5). Experimental observation of the intake process at different engine speeds has shown that the pressure in the intake pipe will oscillate at a frequency that is the integer multiple of the cycle frequency nearest to the lowest ¼ wavelength resonant frequency of the pipe.

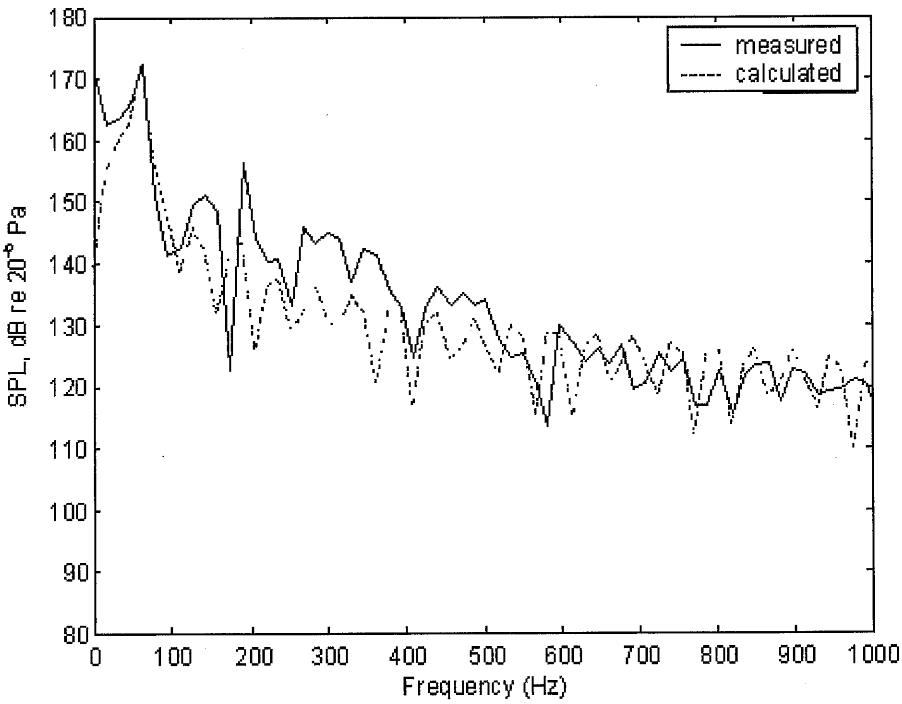

Figure: 8 Calculated and measured sound pressure level spectra in the intake port at 2000 revmin^{-1}.

5. MULTIPLE CYLINDER MODELS

The discussion so far has been restricted to the single cylinder engine. However, the calculation procedure can be extended to include multiple cylinder engines once a suitable intake manifold model is developed.

The intake manifold has two effects on the performance and intake noise obtained from an engine. Firstly, the complex network of pipes results in more acoustic resonances than are found with single pipe lengths. This alters the frequencies at which the intake wave oscillates. Secondly, the acoustic waves generated by each cylinder can interact in the manifold. This latter effect has been demonstrated experimentally [1].

A linear plane wave acoustic model for intake manifolds has been developed [5]. This comprises models for pipe lengths with open ends, pipe lengths with closed ends, sudden

expansions, sudden contractions and junctions involving three or more pipes of differing sizes. Each model has been found to validate well against two-transducer wave decomposition measurements made on the bench using full scale plastic components.

The various models can be assembled to describe almost any practical manifold geometry. One such assemblage is shown in Figure: 9 where a typical end feed plenum type manifold is assembled from a sequence of pipes and junctions.

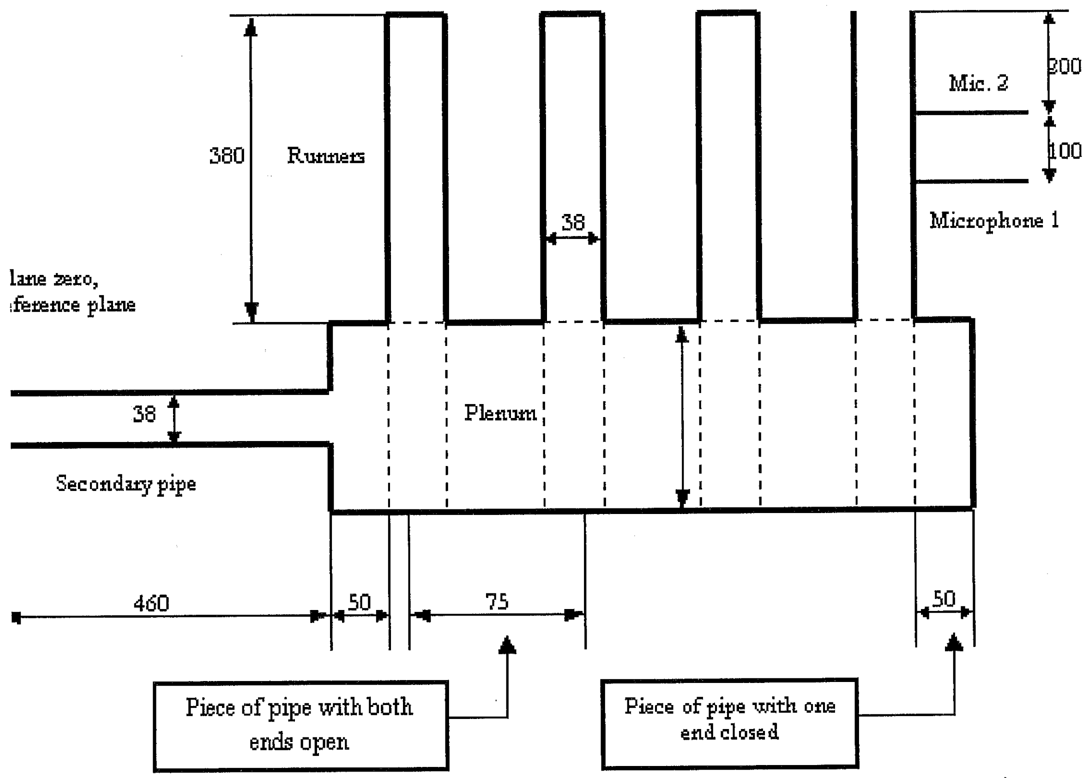

Figure: 9 An end feed plenum type intake manifold. Dimensions are in millimetres.

Assuming that only one intake valve is open at any given time (an acceptable assumption for regular road-going four cylinder engines) then Figure: 9 shows the acoustic model for the load impedance Z_1 at the end cylinder of a bank of four. Different models are required for the other three cylinders, where the appropriate 'runner' is open at both ends and all the others are shut at the valve position.

Figure: 10 shows the specific acoustic impedance ratio calculated and measured at a position corresponding to the end cylinder of Figure: 9. Measured results have been obtained using the two-transducer wave decomposition technique on a bench with zero flow and a full size plastic model of the intake manifold. The calculated results were obtained using the linear acoustic model [5].

The agreement between measured and calculated results is fair at frequencies below 1000 Hz. It was found that the calculated results were very sensitive to the dimensions of the pipework around junctions. It was also found that the end-corrections commonly used in the description of the acoustic transfer at sudden changes in cross sectional area [1] were not suitable when several changes in cross sectional area occurred near to each other as in the case of the four tightly packed junctions seen at the plenum in Figure: 9.

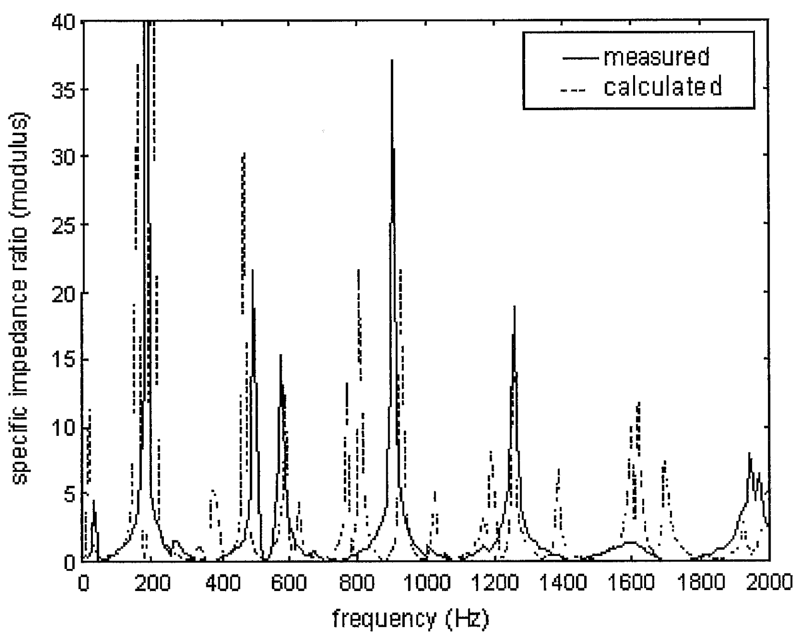

Figure: 10 Calculated and measured specific impedance ratio for an end feed plenum type intake manifold.

The multiple cylinder results shown are work in progress. The calculation of the acoustic wave in each port of a multiple cylinder engine is possible if a different acoustic model for the load impedance Z_1 is used for each cylinder. Then equations 6 and 13 can be used to calculate pressure time histories at each port as if they were independent of each other. If these time histories are phased with respect to each other according to the firing pattern of the engine and then summed, the interaction between cylinders will be accounted for.

CONCLUSIONS

The intake process of a single cylinder engine has been considered in some detail. A linear plane wave acoustic model has been constructed that can account for the influence of engine geometry, engine operating conditions and intake pipe acoustics on the volumetric efficiency and intake noise of practical engines.

The acoustic model has been shown to produces predictions of the acoustic wave in the intake port of a single cylinder engine that agree well with measurement. This lends support to the adoption of two simplifying assumptions in the calculations. The first relates to the way in which the acoustic source and load are assumed to be coupled, and the second relates to the assumption of a very high source impedance at all times.

The success of the model suggests that it could be used as part of an iterative gas-dynamic calculation to yield improved predictions of engine performance. It has been shown to give good predictions of intake noise spectrum and level in its own right.

The acoustic model can be extended to consider multiple cylinder engines with the adoption of a linear acoustic model for the often complex intake manifold. The interaction between the acoustic waves originating from the different cylinders can be accounted for. The completion of such a calculation procedure is work in progress.

ACKNOWLEDGEMENTS

The authors gratefully acknowledge the support of EPSRC under Grant No. GR/R04324 for this work. The MSc thesis work of several Cranfield University students has also contributed to the timely delivery of the objectives of GR/R04324, and so acknowledgement is given to Iciar De Soto, Sotiris Gritsis, Ruben Perez Arenas and Pedro Rubio Unzueta.

REFERENCES

1 A. Ohata, Y. Ishida
Dynamic inlet pressure and volumetric efficiency of four cycle four cylinder engine
SAE Paper No. 820407
1982

2 D.E. Winterbone, R.J. Pearson
Design techniques for engine manifolds – wave action methods for IC engines
Professional Engineering Publishing
1999

3 P.O.A.L. Davies
Practical flow duct acoustics
Journal of Sound and Vibration, 124(1), 91-115

1988

4 P.L. Rubio Unzueta
Quantifying throttle losses
MSc. Thesis, Cranfield University
2001

5 Iciar De Soto
The acoustics of internal combustion engine manifolds
MSc. Thesis, Cranfield University
2001